

# Amyloid $\beta$ oligomers induce interleukin-1 $\beta$ production in primary microglia in a cathepsin B- and reactive oxygen species-dependent manner

*Jun Taneo<sup>1</sup>, Takumi Adachi<sup>1</sup>, Aiko Yoshida<sup>2</sup>, Kunio Takayasu<sup>2</sup>, Kazuhiko Takahara<sup>1, 3, \*</sup>, and Kayo Inaba<sup>1, 3</sup>*

<sup>1</sup>Department of Animal Development and Physiology, Kyoto University, Yoshida-Konoe, Sakyo, Kyoto 606-8501, Japan; <sup>2</sup>Responses to Environmental Signals and Stresses, Graduate School of

Biostudies, Kyoto University, Yoshida-Konoe, Sakyo, Kyoto, Kyoto 606-8501, Japan; and

<sup>3</sup>Japan Science and Technology Agency, Core Research for Evolutional Science and Technology (CREST), Tokyo 102-0081, Japan

**\*Corresponding author** Dr. Kazuhiko Takahara, Laboratory of Immunobiology, Department of Animal Development and Physiology, Division of Systemic Life Science, Graduate School of Biostudies, Kyoto University, Yoshida-Konoe, Sakyo, Kyoto 606-8501, Japan

Phone: +81-75-753-4106, Fax: +81-75-753-4112, E-mail: ktakahar@zoo.zool.kyoto-u.ac.jp

## **Abbreviations**

A $\beta$ , amyloid  $\beta$ ; AD, Alzheimer's disease; AFM, atomic force microscopy; BMDM, bone marrow-derived macrophages; DAPI, 4'-diamidino-2-phenylindole; IL-1 $\beta$ , interleukin-1 $\beta$ ; LPS, lipopolysaccharide; LxB, latex beads; ROS, reactive oxygen species

## **Abstract**

Amyloid  $\beta$  (A $\beta$ ) peptide, a causative agent of Alzheimer's disease, forms two types of aggregates: oligomers and fibrils. These aggregates induce inflammatory responses, such as interleukin-1 $\beta$  (IL-1 $\beta$ ) production by microglia, which are macrophage-like cells located in the brain. In this study, we examined the effect of the two forms of A $\beta$  aggregates on IL-1 $\beta$  production in mouse primary microglia. We prepared A $\beta$  oligomer and fibril from A $\beta$  (1–42) peptide *in vitro*. We analyzed the characteristics of these oligomers and fibrils by electrophoresis and atomic force microscopy. Interestingly, A $\beta$  oligomers but not A $\beta$  monomers or fibrils induced robust IL-1 $\beta$  production in the presence of lipopolysaccharide. Moreover, A $\beta$  oligomers induced endo/phagolysosome rupture, which released cathepsin B into the cytoplasm. A $\beta$  oligomer-induced IL-1 $\beta$  production was inhibited not only by the cathepsin B inhibitor CA-074-Me but also by the reactive oxygen species (ROS) inhibitor N-acetylcysteine. Random chemical crosslinking abolished the ability of the oligomers to induce IL-1 $\beta$ . Thus, multimerization and fibrillization causes A $\beta$  oligomers to lose the ability to induce IL-1 $\beta$ . These results indicate that A $\beta$  oligomers, but not fibrils, induce IL-1 $\beta$  production in primary microglia in a cathepsin B- and ROS-dependent manner.

**Keywords:** AFM, amyloid  $\beta$ , fibrils, IL-1 $\beta$ , microglia, oligomers

## 1. Introduction

Amyloid  $\beta$  ( $A\beta$ ) peptides form aggregates that accumulate in senile plaques within the brain tissue of patients with Alzheimer's disease (AD). This phenomenon is the pathologic hallmark of AD [1].  $A\beta$  forms 2 distinct types of aggregates, soluble  $A\beta$  oligomers and insoluble  $A\beta$  fibrils (see ref. [2]). Both types of  $A\beta$  aggregates seem to induce production of the inflammatory cytokine IL-1 $\beta$  *via* NOD-like receptor family, pyrin domain containing 3 (NLRP3) an inflammasome protein. IL-1 $\beta$  is one of the most prominently expressed cytokines in brain tissue of AD patients, and it is thought to cause neurodegeneration [3].

Induction of IL-1 $\beta$  requires 2 sequential signals [4]. The first signal is transduced through toll-like receptors (*e.g.*, TLR4) and leads to the production of the pro-form of IL-1 $\beta$ . The second signal occurs *via* inflammasome activation, which requires lysosomal cathepsin B [5,6] and reactive oxygen species (ROS) [7,8].  $A\beta$  aggregates as well as small particles such as asbestos lead to cathepsin B leakage from phagolysosomes, which binds directly to NLRP3 and activates it [9]. In addition, the  $A\beta$  aggregates/particles also induce mitochondrial damage and subsequent ROS production [8], leading to activation of the NLRP3 inflammasome [10]. After activation, the NLRP3 inflammasome facilitates activation of caspase-1, and then pro-IL-1 $\beta$  is processed to its bioactive form [11].

Microglia reside in the brain [12] and monitor the functional status of neuronal cells, tissue metabolism, inflammation, and cell death [13]. The inflammatory and immunological processes mediated by microglia are thought to play a pivotal role in the initiation and progression of AD [14] since activated microglia are recruited to senile plaques where they phagocytose  $A\beta$  and secrete IL-1 $\beta$ .

Although it has been shown that A $\beta$  aggregates induce IL-1 $\beta$  [5], which types of aggregates induce IL-1 $\beta$  production by primary microglia remains controversial. In this study, we examined which types of aggregates induce IL-1 $\beta$  production by primary microglia by generating size/shape-defined A $\beta$  preparations with low cross-contamination between oligomer and fibril forms.

## **2. Materials and methods**

### *2.1. Mice*

BALB/c mice were purchased from Japan SLC (Hamamatsu, Japan) and were housed and bred under specific pathogen-free conditions. All animal experiments were performed in accordance with the Kyoto University Institutional Guidelines for Animal Use and Experimentation.

### *2.2. Antibodies and reagents*

Purified anti-mouse IL-1 $\beta$  monoclonal antibody (B122) and biotinylated anti-rat IgG2b $\kappa$  were purchased from BD Biosciences (San Jose, CA). Biotinylated anti-IL-1 $\beta$  and FITC-labeled anti-rabbit antibodies were purchased from eBioscience (San Diego, CA) and Jackson ImmunoResearch (West Grove, PA), respectively. Rabbit anti-A $\beta$  antibody and Alexa-647-conjugated anti-Lamp1 monoclonal antibody (1D4B) were purchased from Cell Signaling Technology (Danvers, MA) and BioLegend (San Diego, CA), respectively. RPMI1640 and DMEM were purchased from Invitrogen (Carlsbad, CA), and ultra-pure LPS (*E. coli* 0111:B4) was purchased from InvivoGen (San Diego, CA). N-acetylcysteine (NAC) and Ham's F-12 were

purchased from Sigma-Aldrich (St. Louis, MO), and the cathepsin B inhibitor CA-074-Me was purchased from Calbiochem (Darmstadt, Germany).

### *2.3. Preparations of A $\beta$ oligomers and fibrils*

A $\beta$  oligomers and fibrils were prepared from A $\beta$ (1–42) peptides (Peptide Institute, Osaka, Japan) as previously described [15] with some modifications (see Fig. S1). To prepare A $\beta$  oligomers, peptide dissolved in dimethyl sulfoxide (DMSO; Sigma-Aldrich) was diluted in phenol red-free RPMI1640 and incubated for 24 h at 4°C. To prepare A $\beta$  fibrils, the peptide solution was diluted with 100 mM HCl (instead of 10 mM HCl) and then incubated for 24 h at 37°C. The fibril preparation was then centrifuged, and the resulting pellet was washed and resuspended in phenol red-free RPMI1640. The washing step was repeated 3 times to remove A $\beta$  oligomers. To prepare A $\beta$  monomers, the peptide solution was diluted with phenol red-free RPMI1640, ultrasonicated for 10 min, and then passed through a 0.22- $\mu$ m membrane filter (Millipore, Billerica, MA).

### *2.4. AFM imaging and analysis*

The AFM analysis was performed as described previously [16]. The A $\beta$  samples were prepared by diluting the preformed A $\beta$  solution with PBS to 10 nM. Aliquots of the diluted samples (20  $\mu$ L) were spotted on freshly cleaved mica and incubated at room temperature (RT) for 10 min. In some cases, the mica surface was first treated with 10 mM spermidine (Nacalai Tesque, Kyoto, Japan) for 10 min prior to spotting of the sample.

Atomic force microscopy (AFM) images were obtained with a Multimode AFM equipped with a Nanoscope III or IV controller and a J scanner (Digital Instruments, Inc., Santa Barbara,

CA). The microscope was operated in Tapping Mode™ at a scanning rate of 1.0–2.0 Hz with 512 × 512 pixels. Rectangular silicon cantilevers with sharpened tetrahedral tips were used (OMCL AC160TS; Olympus, Japan). The probes had a tip radius of approximately 7 nm, a resonant frequency of about 300 kHz, and a spring constant of about 26 N/m. Images shown were flattened with Nanoscope (v.5.31 r1) software and exported as tiffs. The flattened SPM images were opened in Gwyddion (Department of Metrology, Czech Metrology Institute, Czech Republic) and analyzed. Aβ molecules or fibrils were marked by selecting all molecules or fibrils above a 0.10–0.20-nm threshold. The distributions of various grain characteristics were then exported as a raw data file, and then the “measure individual grain” tool was used to select each molecule and record the zero basis volume ( $V_c$ ) and maximum height of each molecule or fibril. The values were entered into Origin Lab software (OriginLab Corp., USA), plotted as histograms, and fitted with Gaussian curves to obtain the center value for each histogram. The errors are reported as the standard deviation of the Gaussian distribution. The contour length of the Aβ fibrils was measured with Nanoscope software. These analyses were performed in at least 3 random fields.

### *2.5. Silver staining*

Aβ preparations were separated by SDS-PAGE in 4–20% Mini-PROTEAN TGX Precast Gels (Bio-Rad, Hercules, CA) and visualized using the Silver Staining Kit, Protein (GE Healthcare, Pittsburgh, PA).

### *2.6. Protein quantification of the Aβ preparations*

The protein content of the A $\beta$  preparations was quantified by Lowry's method [17] prior to each experiment. In some cases, the proportion of each A $\beta$  form was estimated using ImageJ software (NIH, Bethesda, MD) by scanning the SDS-PAGE gel after silver staining. The number of large fibrils present in each preparation was calculated by subtracting the number of pixels representing monomers and oligomers from the total number of pixels in the preparation.

### *2.7. Preparation of primary microglia and cytokine production assay*

Primary microglia were isolated as described previously [18]. Brain tissues from 5-day postnatal mouse pups were used. After digestion, the cell pellet was resuspended in DMEM:Ham's F-12 (1:1) supplemented with 10% FCS, 100 U/mL penicillin, and 100  $\mu$ g/mL streptomycin (DF-10). Cells were seeded into flasks at  $1.0\text{--}2.0 \times 10^7$  cells/75 cm<sup>2</sup>. The medium was changed every 2 to 3 days. Ten days later, the flasks were shaken gently for 2 min, and then the floating cells were collected. As determined by flow cytometry, over 90% of the floating cells were CD11b<sup>+</sup> CD45<sup>low</sup> microglia.

Microglia were plated at a density of  $2.5 \times 10^4$  cells/100  $\mu$ L/well into 96-well tissue culture plates and stimulated with the A $\beta$  preparations in the presence of 100 ng/mL LPS for 24 h. In some experiments, cells were incubated with 5  $\mu$ M CA-074-Me and 2.5 mM NAC for 1 h before stimulation. Then, IL-1 $\beta$  production was determined by ELISA, and the production of other cytokines was assessed using a cytometric bead array (BD Biosciences).

### *2.8. Immunostaining and microscopic analysis*

After 2 h of incubation on poly-L-lysine-coated cover slips, adherent microglia ( $3.0 \times 10^4$ ) were stimulated as described above. The cells were then fixed with 1% glutaraldehyde in PBS

for 20 min and incubated with 0.1% saponin for 20 min. Specimens were then treated with an anti-CD32/64 antibody and incubated with an anti-A $\beta$  antibody and a FITC-anti-rabbit antibody. Next, they were incubated with an Alexa-647-conjugated anti-Lamp-1 antibody and stained with 4'-diamidino-2-phenylindole (Molecular Probes, Eugene, OR) for 20 min. Specimens were observed using a deconvolution microscope (BX51-FL; Olympus) and SlideBook imaging software (Intelligent Imaging Innovation, Denver, CO).

### *2.9. Detection of cathepsin B leakage from endo/phagolysosomes*

Cellular localization of active cathepsin B was monitored using a fluorescent cathepsin B substrate (Magic Red; Immunochemistry Technologies, Bloomington, MN). After incubation for 2 h in glass-bottom dishes (at a density of  $4.0 \times 10^4$  cells/well), microglia were stimulated for 24 h as described above. Magic Red was added to the culture and incubated for the last 20 min according to the manufacturer's protocols. The cells were then observed using a BZ-8000 BioZero live-cell imaging device (Keyence, Osaka, Japan).

### *2.10. A $\beta$ oligomer crosslinking*

A $\beta$  oligomer prepared in PBS was crosslinked using 2 mM ethylene glycol bis(sulfosuccinimidylsuccinate) (sulfo-EGS, Thermo Scientific Pierce, Rockford, IL) at room temperature for 45 min and then quenched with 20 mM Tris-HCl (pH 7.2). The preparations were dialyzed against PBS before use.

### *2.11. Statistical analysis*



Data are expressed as the mean (SD) of triplicate cultures. Statistical significance was determined using a two-tailed Student's *t*-test. All experiments were performed at least twice, and representative results are shown.

### 3. Results

#### 3.1. Preparation and characterization of A $\beta$

Monomer, oligomer, and fibril A $\beta$  preparations were obtained as shown in Fig. S1. All 3 preparations were analyzed by SDS-PAGE and silver staining (Fig. 1A, B). The oligomer preparation contained 2 types of A $\beta$  aggregates as well as monomers, whereas the fibril preparation contained large fibrillar aggregates that could not penetrate the polyacrylamide gel. The fibril preparation also contained monomers and a very small amount of oligomers (Fig. 1B). The gel scanning results (Fig. 1C, D) showed that the monomer preparation contained less than 20% oligomer contaminants and the oligomer preparation consisted of approximately 40% oligomers and 60% monomers (Fig. 1E). The fibril preparation contained approximately 2/3 fibrils and 1/3 monomers, with a very small amount of oligomers.

The sizes and shapes of the A $\beta$  preparations were further analyzed using AFM. The oligomer preparation contained globular structures with an average *z*-height of  $0.4 \pm 0.2$  nm but no fibril structures (Fig. 1F, *left panels*). SDS-PAGE and AFM showed that the A $\beta$  trimers/tetramers formed large complexes, such as A $\beta$ -derived diffusible ligands (ADDLs) [19]. In contrast, the fibril preparation contained long fiber structures (Fig. 1F, *right panels*). There are 2 types of A $\beta$  fibrils, type I and type II [20]. The mean *z*-height of the predominant fibril form was  $4.1 \pm 0.5$  nm, and most fibrils were 246–719 nm in length. Therefore, this fibril preparation contained mostly type II fibrils.

### *3.2. Uptake of A $\beta$ aggregates and subsequent IL-1 $\beta$ production by primary microglia*

Next, we monitored A $\beta$  uptake from the 3 different A $\beta$  preparations by primary microglia. Immunofluorescence staining with an anti-A $\beta$  antibody showed that, A $\beta$  aggregates from both the oligomer and fibril preparations were internalized by microglia, and they produced punctuate and diffuse signals, respectively (Fig. 2A). In contrast, little signal was observed when the monomer A $\beta$  preparation was used.

We next examined the effect of the A $\beta$  preparations on IL-1 $\beta$  production in primary microglia. We found that the oligomer preparation, but not the monomer or fibril preparation, induced robust IL-1 $\beta$  production in the presence of LPS when the preparations were used at a concentration of 10  $\mu$ M (Fig. 2B). TNF- $\alpha$  and MCP-1 production in response to LPS were not reduced by addition of the A $\beta$  preparations (Fig. S2). Thus, the possibility that the A $\beta$  preparations caused heavy cellular damage could be excluded. The oligomer preparation also evoked much greater IL-1 $\beta$  production in bone marrow-derived macrophages (BMDMs) than the fibril preparation (Fig. S3). These results indicate that A $\beta$  oligomers induce IL-1 $\beta$  production more efficiently than A $\beta$  fibrils.

### *3.3. Cathepsin B and ROS are required for IL-1 $\beta$ production by microglia*

We previously showed that IL-1 $\beta$  production by BMDMs in response to nano-sized latex beads (LxB) in the presence of LPS was dependent on cathepsin B and that microglia also produced IL-1 $\beta$  in response to nano-sized LxB [21]. Therefore, A $\beta$ -induced IL-1 $\beta$  production may occur *via* a similar mechanism. To address this question, we first checked whether microglia respond to LxB in a cathepsin B-dependent manner (Fig. S4). Leakage of cathepsin B into the

cytoplasm was only detected when microglia were cultured with 20 nm LxB, but not with 1,000 nm LxB (Fig. S4B). Furthermore, addition of the cathepsin B inhibitor CA-074-Me (5  $\mu$ M) suppressed 20 nm LxB-induced IL-1 $\beta$  production, although the inhibitor did not affect TNF- $\alpha$  induction (Fig. S4B). In contrast, the ROS inhibitor NAC (2.5 mM) did not affect IL-1 $\beta$  production in response to 1,000 nm or 20 nm LxB (data not shown). These results suggest that microglia produce IL-1 $\beta$  in response to 20 nm LxB in a cathepsin B-dependent manner, as was observed in BMDMs.

We next checked whether A $\beta$  oligomer-induced IL-1 $\beta$  production is dependent on cathepsin B. As shown in Fig. 3A, release of activated cathepsin B into the cytoplasm was observed only when microglia were stimulated with the oligomer preparation. When the cells were stimulated with the fibril preparation, active cathepsin B was mainly observed as punctate structures, which could be endo/phagolysosomes, but it was not observed in the cytoplasm. Moreover, the cathepsin B inhibitor significantly reduced oligomer-induced IL-1 $\beta$  production (Fig. 3B, *left panel*), but did not affect TNF- $\alpha$  production (Fig. 3B, *right panel*). These results indicate that, similar to 20 nm LxB, A $\beta$  oligomers induce IL-1 $\beta$  production by microglia in a cathepsin B-dependent manner. The ROS inhibitor NAC (2.5 mM) unexpectedly suppressed IL-1 $\beta$  production (Fig. 3C), which is not consistent with the results obtained with BMDMs and LxB. In BMDMs, IL-1 $\beta$  production in response to 20 nm LxB was dependent on cathepsin B but independent of ROS [21].

#### *3.4. Induction of IL-1 $\beta$ by crosslinked A $\beta$ oligomer*

It is likely that the difference in shape between the A $\beta$  oligomer and fibril leads affects the ability to induce IL-1 $\beta$ . However, the form of the fibril involved in alternation of IL-1 $\beta$  induction

is not clear. To investigate this, an oligomer preparation was further crosslinked with sulfo-EGS. Crosslinking of the A $\beta$  oligomers generated high molecular weight (>225 kDa) aggregates (Fig. 4A). The aggregates were globular rather than fibrillar in structure with an average diameter of  $5.3 \pm 0.9$  nm (Fig. 4B). Analysis of the volume distribution of the cross-linked oligomers by AFM showed 2 average sizes,  $1,373 \pm 1,418$  nm<sup>3</sup> and  $3,498 \pm 2,250$  nm<sup>3</sup> (Fig. S5), corresponding to ~180 and ~460 A $\beta$  peptides, respectively. We then examined the ability of the crosslinked preparations to induce IL-1 $\beta$  (Fig. 4C), the crosslinked preparation significantly reduced IL-1 $\beta$  induction compared to that induced by the oligomer preparation. This result suggests that increasing the size of the A $\beta$  aggregates, either by generating fibrils or by crosslinking oligomers, abolishes the ability of the aggregates to induce IL-1 $\beta$  production.

#### **4. Discussion**

In this study, we showed that microglia produce IL-1 $\beta$  in response to A $\beta$  oligomer in a cathepsin B- and ROS-dependent manner. These results along with the involvement of IL-1 $\beta$  in AD [3] are consistent with the observation that treatment with cathepsin [22] and ROS [23] inhibitors improves AD symptoms.

Both 20 nm LxB and A $\beta$  oligomer induced leakage of cathepsin B, suggesting that small sized particles/aggregates cause rupture of endo/phagolysosomes and subsequent IL-1 $\beta$  production. These results are consistent with those obtained with BMDMs and LxB [21]. However, A $\beta$  oligomer-induced IL-1 $\beta$  production by microglia is also ROS inhibitor-sensitive. In BMDMs, IL-1 $\beta$  is produced in response to 20 nm LxB independent of ROS [21]. Exposure to 20 nm LxB caused strong mitochondria damage, leading to their clearance, which resulted in

downregulation of ROS production [21]. Therefore, unlike LxB, A $\beta$  oligomers may not induce strong mitochondria damage. Consequently, ROS-producing mitochondria remain in the cells.

A large surface area is thought to be important for the bioactivity/toxicity of small particles [24]. Since A $\beta$  fibrils have much less surface area than oligomers do, it is thought large A $\beta$  aggregates, such as fibrils, do not promote AD and may even be protective against progression of AD [2]. This idea was supported by studies on other protein-aggregating disorders such as Huntington's disease [25]. Our data are consistent with this hypothesis because only A $\beta$  oligomers but not fibrils or crosslinked oligomers induced IL-1 $\beta$  production. It is likely that crosslinking of A $\beta$  oligomers decreases their surface area due to the formation of large molecular aggregates, resulting in the loss of IL-1 $\beta$  induction ability.

Recent studies have shown that, in addition to ADDLs, there are several soluble A $\beta$  preparations, such as A $\beta$ \*56 and A $\beta$ O as well as the protofibril A $\beta$ 42CC [26]. These A $\beta$  fibrillar intermediates are composed of different numbers of A $\beta$  peptides and have diverse sizes, shapes, and biological effects. In regards to possible species and structural specificity, it should be noted that Parajuli *et al.* reported ROS-dependent but cathepsin B-independent IL-1 $\beta$  production in mouse primary microglia upon stimulation with A $\beta$  oligomers [27]. At present, the reason for this discrepancy is not clear, because no precise information about the size/shape of their oligomer preparations was provided. One possible explanation is that the oligomers used in those studies had different compositions or structures than the ones that we used.

## **Acknowledgments**

This work was supported in part by a Grant-in-Aid for Scientific Research (21590417 to K. Takahara), a Grant-in-Aid for Challenging Exploratory Research (20659036 to K. I.) from Core

Research for Evolutional Science and Technology, Japan Science and Technology Agency (100111500004 to K. I.), and by a grant from the Shimizu Foundation for Immunology and Neuroscience in 2013 (to K. Takahara).

## References

- [1] S. Singh, A. Kushwah, R. Singh, M. Farswan, R. Kaur, Current therapeutic strategy in Alzheimer's disease, *Eur. Rev. Med.* 16 (2012) 1651-1664.
- [2] C. Haass, D. Selkoe, Soluble protein oligomers in neurodegeneration: lessons from the Alzheimer's amyloid  $\beta$ -peptide, *Nat. Rev. Mol. Cell Biol.* 8 (2007) 101-112.
- [3] Y.-J. Lee, S. Han, S.-Y. Nam, K.-W. Oh, J. Hong, Inflammation and Alzheimer's disease, *Arch. Pharm. Res.* 33 (2010) 1539-1556.
- [4] L. Franchi, R. Munoz-Planillo, G. Nunez, Sensing and reacting to microbes through the inflammasomes, *Nat. Immunol.* 13 (2012) 325-332.
- [5] A. Halle, V. Hornung, G. Petzold, C. Stewart, B. Monks, T. Reinheckel, K. Fitzgerald, E. Latz, K. Moore, D. Golenbock, The NALP3 inflammasome is involved in the innate immune response to amyloid- $\beta$ , *Nat. Immunol.* 9 (2008) 857-865.
- [6] K. Rajamäki, J. Lappalainen, K. Oörni, E. Välimäki, S. Matikainen, P. Kovanen, K. Eklund, Cholesterol crystals activate the NLRP3 inflammasome in human macrophages: a novel link between cholesterol metabolism and inflammation, *PLoS One* 5 (2010) e11765.
- [7] S. Cassel, S. Eisenbarth, S. Iyer, J. Sadler, O. Colegio, L. Tephly, A. Carter, P. Rothman, R. Flavell, F. Sutterwala, The Nalp3 inflammasome is essential for the development of silicosis, *Proc. Natl. Acad. Sci. USA* 105 (2008) 9035-9040.
- [8] K. Nakahira, J. Haspel, V. Rathinam, S.-J. Lee, T. Dolinay, H. Lam, J. Englert, M.

- Rabinovitch, M. Cernadas, H. Kim, K. Fitzgerald, S. Ryter, A. Choi, Autophagy proteins regulate innate immune responses by inhibiting the release of mitochondrial DNA mediated by the NALP3 inflammasome, *Nat. Immunol.* 12 (2011) 222-230.
- [9] M. Bruchard, G. Mignot, V. Derangère, F. Chalmin, A. Chevriaux, F. Végran, W. Boireau, B. Simon, B. Ryffel, J. Connat, J. Kanellopoulos, F. Martin, C. Rébé, L. Apetoh, F. Ghiringhelli, Chemotherapy-triggered cathepsin B release in myeloid-derived suppressor cells activates the Nlrp3 inflammasome and promotes tumor growth, *Nat. Med.* 19 (2013) 57-64.
- [10] R. Zhou, A. Tardivel, B. Thorens, I. Choi, J. Tschopp, Thioredoxin-interacting protein links oxidative stress to inflammasome activation, *Nat. Immunol.* 11 (2010) 136-140.
- [11] B. Davis, H. Wen, J. Ting, The inflammasome NLRs in immunity, inflammation, and associated diseases, *Annu. Rev. Immunol.* 29 (2011) 707-735.
- [12] M. Prinz, J. Priller, S. Sisodia, R. Ransohoff, Heterogeneity of CNS myeloid cells and their roles in neurodegeneration, *Nat. Neurosci.* 14 (2011) 1227-1235.
- [13] K. Saijo, C.K. Glass, Microglial cell origin and phenotypes in health and disease, *Nat. Rev. Immunol.* 11 (2011) 775-787.
- [14] A. Mildner, B. Schlevogt, K. Kierdorf, C. Böttcher, D. Erny, M. Kummer, M. Quinn, W. Brück, I. Bechmann, M. Heneka, J. Priller, M. Prinz, Distinct and non-redundant roles of microglia and myeloid subsets in mouse models of Alzheimer's disease, *J. Neurosci.* 31 (2011) 11159-11171.
- [15] K. Dahlgren, A. Manelli, W. Stine, L. Baker, G. Krafft, M. LaDu, Oligomeric and fibrillar species of amyloid- $\beta$  peptides differentially affect neuronal viability, *J. Biol. Chem.* 277 (2002) 32046-32053.
- [16] F. Pratto, Y. Suzuki, K. Takeyasu, J. Alonso, Single-molecule analysis of protein-DNA

- complexes formed during partition of newly replicated plasmid molecules in *Streptococcus pyogenes*, J. Biol. Chem. 284 (2009) 30298-30306.
- [17] O.H. Lowry, N.J. Rosebrough, A.L. Farr, R.J. Randall, Protein measurement with the Folin phenol reagent, J. Biol. Chem. 193 (1951) 265-275.
- [18] D. Giulian, T. Baker, Characterization of ameboid microglia isolated from developing mammalian brain, J. Neurosci. 6 (1986) 2163-2178.
- [19] M. Lambert, A. Barlow, B. Chromy, C. Edwards, R. Freed, M. Liosatos, T. Morgan, I. Rozovsky, B. Trommer, K. Viola, P. Wals, C. Zhang, C. Finch, G. Krafft, W. Klein, Diffusible, nonfibrillar ligands derived from A $\beta$ 1-42 are potent central nervous system neurotoxins, Proc. Natl. Acad. Sci. USA 95 (1998) 6448-6453.
- [20] J.D. Harper, S.S. Wong, C.M. Lieber, P.T. Lansbury, Observation of metastable A $\beta$  amyloid protofibrils by atomic force microscopy, Chem. Biol. 4 (1997) 119-125.
- [21] T. Adachi, K. Takahara, J. Taneo, Y. Uchiyama, K. Inaba, Particle size of latex beads dictates IL-1 $\beta$  production mechanism, PLoS One 8 (2013) e68499.
- [22] V. Hook, M. Kindy, G. Hook, Inhibitors of cathepsin B improve memory and reduce  $\beta$ -amyloid in transgenic Alzheimer disease mice expressing the wild-type, but not the Swedish mutant,  $\beta$ -secretase site of the amyloid precursor protein, J. Biol. Chem. 283 (2008) 7745-7753.
- [23] M. Dumont, M.F. Beal, Neuroprotective strategies involving ROS in Alzheimer disease, Free Radic. Bio. Med. 51 (2011) 1014-1026.
- [24] G. Oberdörster, E. Oberdörster, J. Oberdörster, Nanotoxicology: an emerging discipline evolving from studies of ultrafine particles, Environ. Health Perspect. 113 (2005) 823-839.
- [25] M. Arrasate, S. Mitra, E. Schweitzer, M. Segal, S. Finkbeiner, Inclusion body formation



reduces levels of mutant huntingtin and the risk of neuronal death, *Nature* 431 (2004) 805-810.

[26] I. Benilova, E. Karran, B. De Strooper, The toxic A $\beta$  oligomer and Alzheimer's disease: an emperor in need of clothes, *Nat. Neurosci.* 15 (2012) 349-357.

[27] B. Parajuli, Y. Sonobe, H. Horiuchi, H. Takeuchi, T. Mizuno, A. Suzumura, Oligomeric amyloid  $\beta$  induces IL-1 $\beta$  processing *via* production of ROS: implication in Alzheimer's disease, *Cell Death Dis.* 4 (2013) e975.

## Figure legends

**Fig. 1.** Preparation and characterization of monomer, oligomer, and fibril forms of A $\beta$ .

(A, B) Silver staining of A $\beta$  preparations after electrophoresis. M, monomers; O, oligomers; F, fibrils. (C and D) Histograms of pixel sizes in the areas depicted in (A and B), respectively. The areas were scanned from the upper side (*top*) to the lower side (*bottom*) of the gel. (E) The percentages of monomers, oligomers, and fibrils in the A $\beta$  preparations. (F) AFM analyses of oligomer (*right panels*) and fibril (*left panels*) preparations. Data represent  $1 \times 1 \mu\text{m}$  for the oligomer preparation and  $2 \times 2 \mu\text{m}$  for the fibril preparation, and 10 nm total *z*-range. Bar graphs show the frequency of each height and length.

**Fig. 2.** Morphological observations and IL-1 $\beta$  production by microglia stimulated with A $\beta$  monomer, oligomer, and fibril preparations.

(A) Microglia on glass coverslips were stimulated with the A $\beta$  preparations in the presence of LPS (100 ng/mL) for 2 h and then stained with anti-A $\beta$  (green), anti-Lamp1 (red), and 4'-diamidino-2-phenylindole (DAPI; blue). BF, bright field. (B) Microglia were stimulated with each A $\beta$  preparation in the presence of LPS for 24 h. IL-1 $\beta$  production was analyzed by ELISA. Bar graphs show the mean (SD) of triplicate cultures. None of the A $\beta$  preparations induced IL-1 $\beta$  production in the absence of LPS.

**Fig. 3.** Leakage of cathepsin B into the cytoplasm and the effects of cathepsin B and ROS inhibitors on IL-1 $\beta$  production by microglia.

(A) Microglia cultured on cover slips were stimulated with the A $\beta$  preparations in the presence of LPS for 24 h and then incubated with a fluorescent cathepsin B substrate for the last 20 min of culture. (B) After treatment with the cathepsin B inhibitor CA-074-Me for 1 h, microglia were stimulated as described in (A). IL-1 $\beta$  and TNF- $\alpha$  production were analyzed by ELISA and cytometric bead array, respectively. (C) After treatment with NAC for 1 h, IL-1 $\beta$  production was analyzed as described in (B). Bar graphs show the mean (SD) of triplicate cultures; nd, not detected; ns, non-sense; \* $p < 0.01$  ( $t$ -test).

**Fig. 4.** Effect of random crosslinking of oligomer preparations on IL-1 $\beta$  production by microglia.

(A) The A $\beta$  oligomer preparation was randomly crosslinked with sulfo-EGS and analyzed by silver staining. (B) The crosslinked preparations were analyzed by atomic force microscopy. Data represent  $1 \times 1 \mu\text{m}$ , and a 10-nm total  $z$ -range. The bar graph shows the frequency of each height. The surface of the mica was treated with spermidine before the preparations were added. (C) Microglia were stimulated with the A $\beta$  preparations in the presence of LPS for 24 h. IL-1 $\beta$  production was analyzed by ELISA. Bar graphs show the mean (SD) of triplicate cultures; \* $p < 0.01$  ( $t$ -test).

Fig.1. Taneo *et al.*

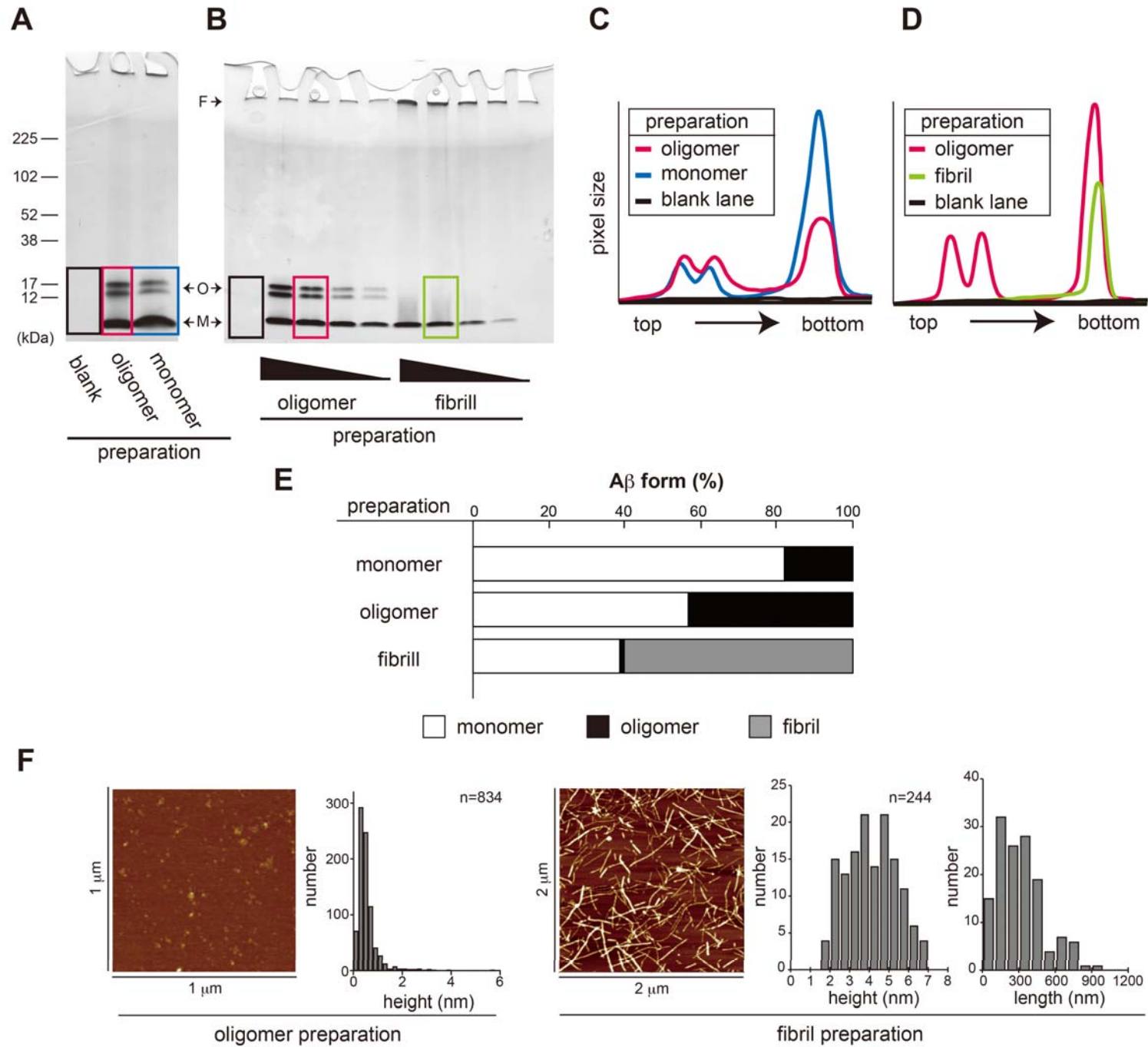
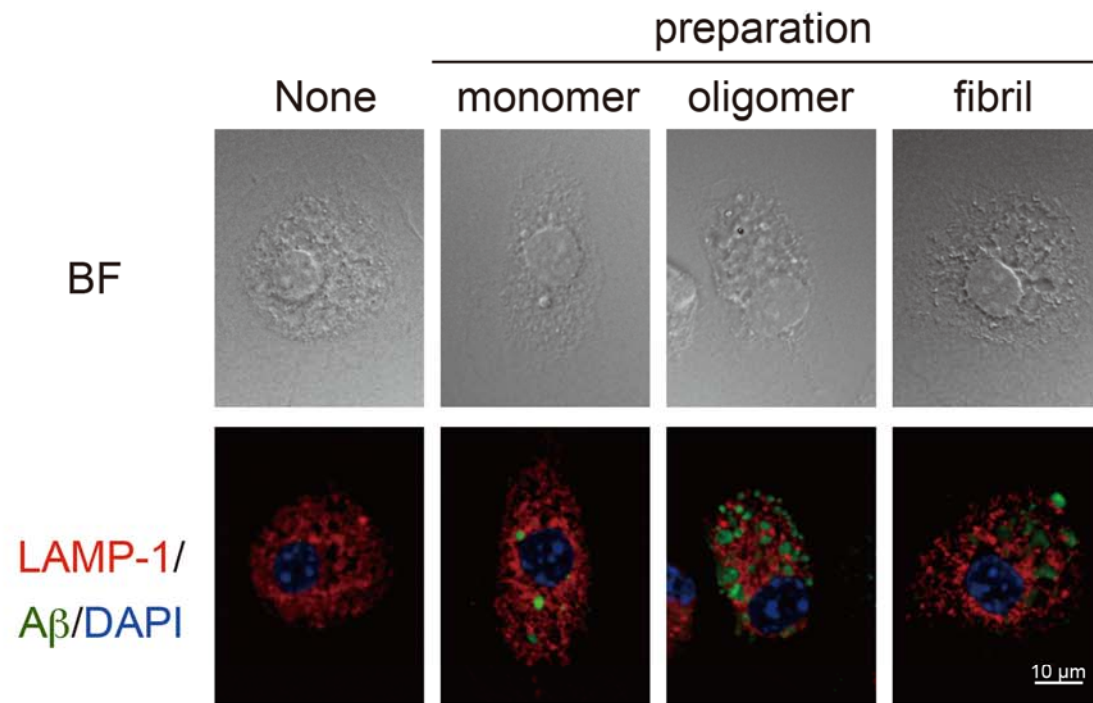


Fig. 2. Taneo *et al.*

**A**



**B**

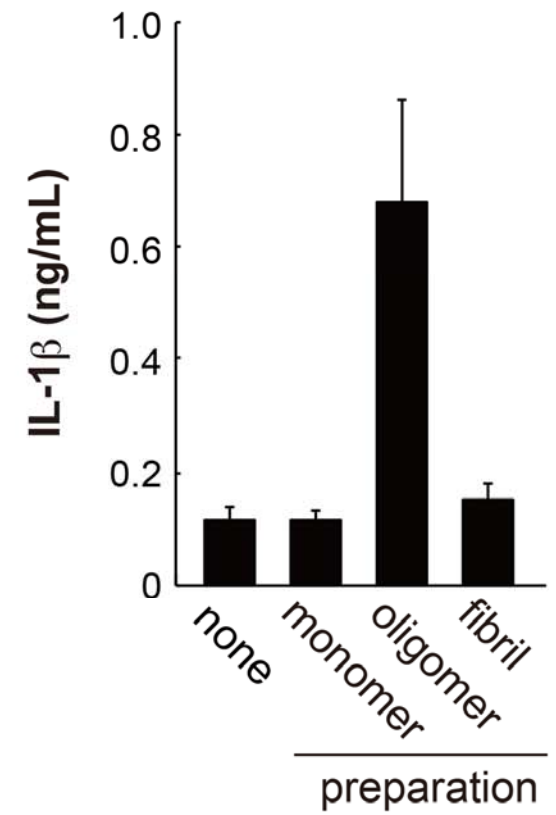


Fig. 3. Taneo *et al.*

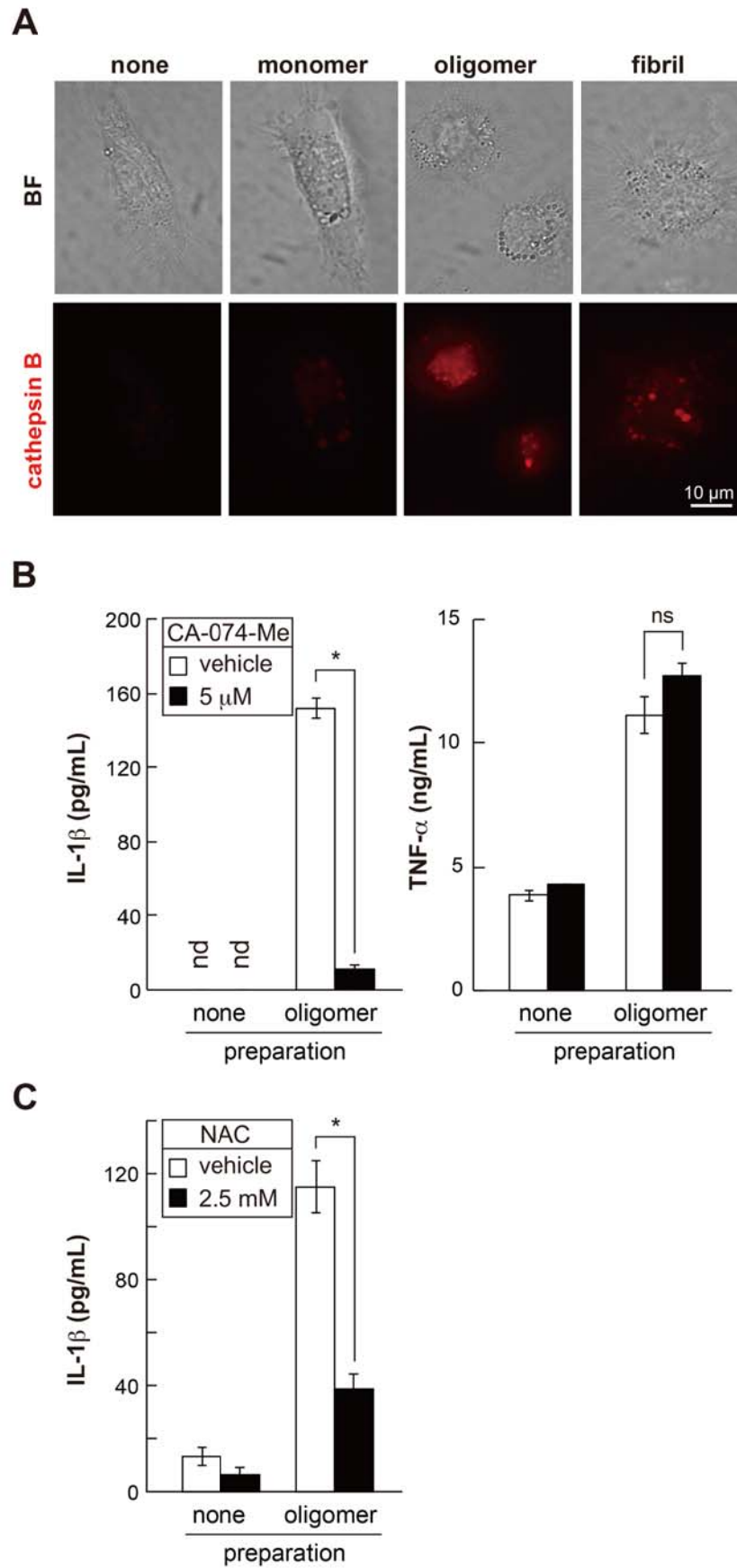
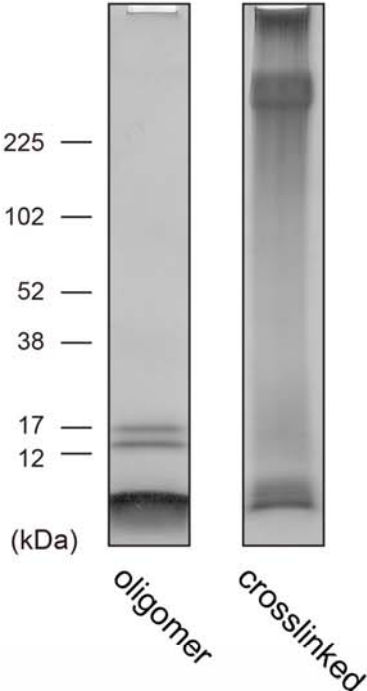
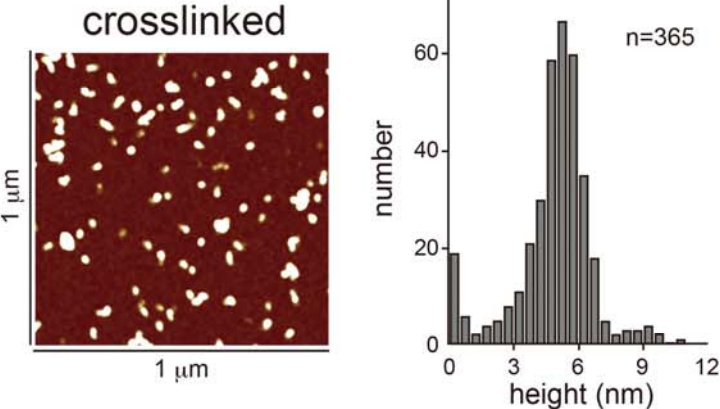


Fig. 4. Taneo *et al.*

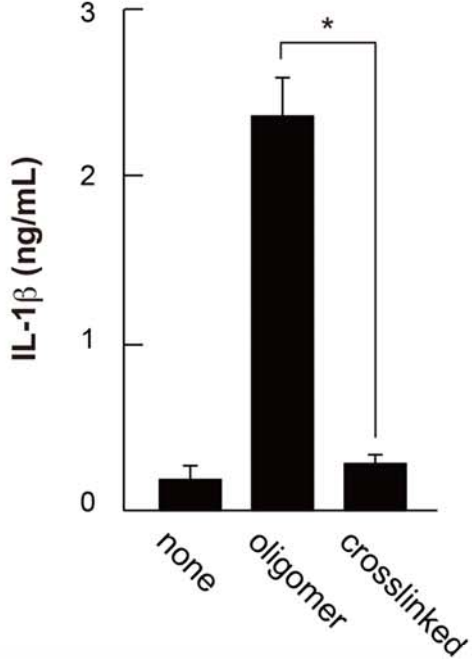
**A**



**B**



**C**



Supplementary information

### **Supplementary methods**

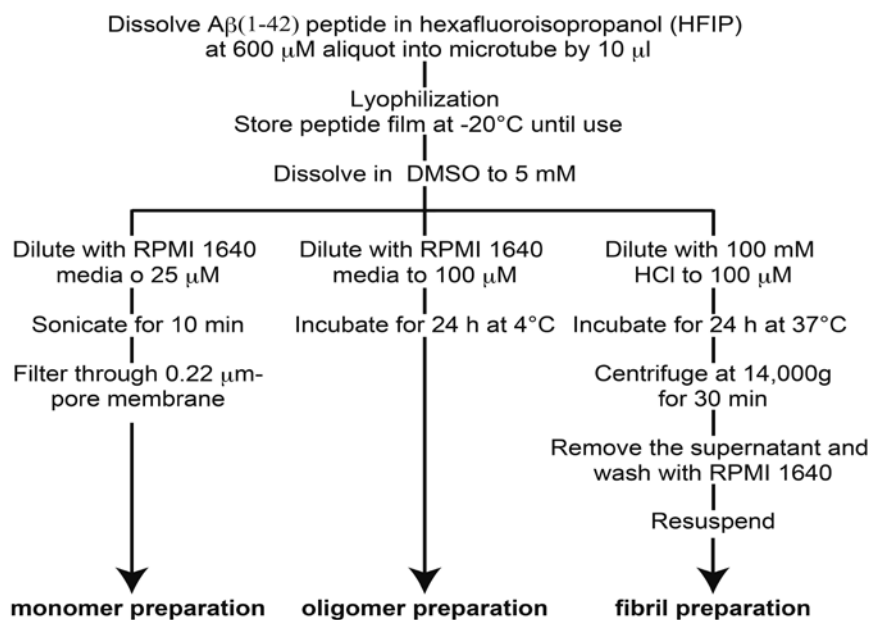
*Stimulation of microglia with latex beads.* Microglia were cultured at a density of  $2.5 \times 10^4$  cells/100  $\mu$ L in 1.5-mL microtubes and stimulated with latex beads (Invitrogen, Carlsbad, CA) at 0.06% (for 1,000-nm diameter beads) or 0.01% (for 20-nm diameter beads) for 9 h in the presence of 10 ng/mL LPS in a stirred culture, as described previously [1].

*Preparation of bone marrow-derived macrophages.* Bone marrow-derived macrophages (BMDMs) were generated by incubating bone marrow cells for 5–6 days in RPMI1640 containing 10% fetal calf serum, 50  $\mu$ M 2-mercaptoethanol, and 15% L929 cell culture supernatant. The cells were stored at  $-80^\circ\text{C}$ . Before use, BMDMs were cultured for 2 days.

*Estimation of molecular weight from AFM data.* The molecular weight of proteins was calculated using the following equation:  $M_0 = V_c N_0 / (V_1 + dV_2)$ , where  $V_c$  is the molecular volume,  $N_0$  is Avogadro's number, and  $V_1$  and  $V_2$  are the partial specific volumes of the individual protein ( $0.74 \text{ cm}^3 \cdot \text{g}^{-1}$  and  $1 \text{ cm}^3 \cdot \text{g}^{-1}$  water, respectively). The extent of protein hydration (0.4 mol  $\text{H}_2\text{O}$ /mol protein) is denoted as  $d$  [2].

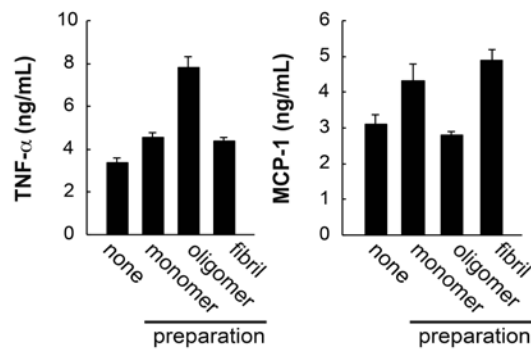


## Supplementary Figures



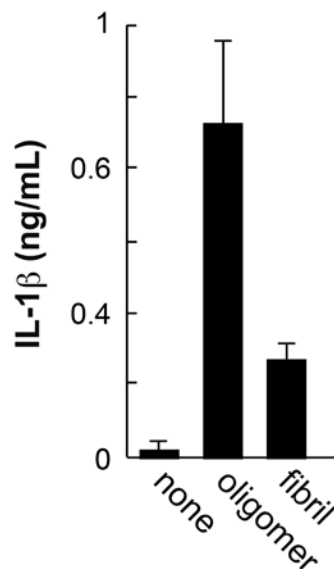
**Supplementary Fig. 1. Schematic diagram of amyloid  $\beta$  aggregate preparations.**

Lyophilized amyloid  $\beta$  ( $A\beta$ ) peptide was dissolved in DMSO and diluted in RPMI to prepare oligomers and in 100 mM HCl to prepare fibrils, and then incubated for 24 h at 24°C and 37°C, respectively. The fibril preparation was centrifuged, and the pellet was suspended in RPMI. For the monomer preparation,  $A\beta$  peptide in DMSO was diluted with RPMI, sonicated, and filtered before use.



**Supplementary Fig. 2. Cytokine production in microglia induced by stimulation with amyloid  $\beta$  preparations in the presence of lipopolysaccharide.**

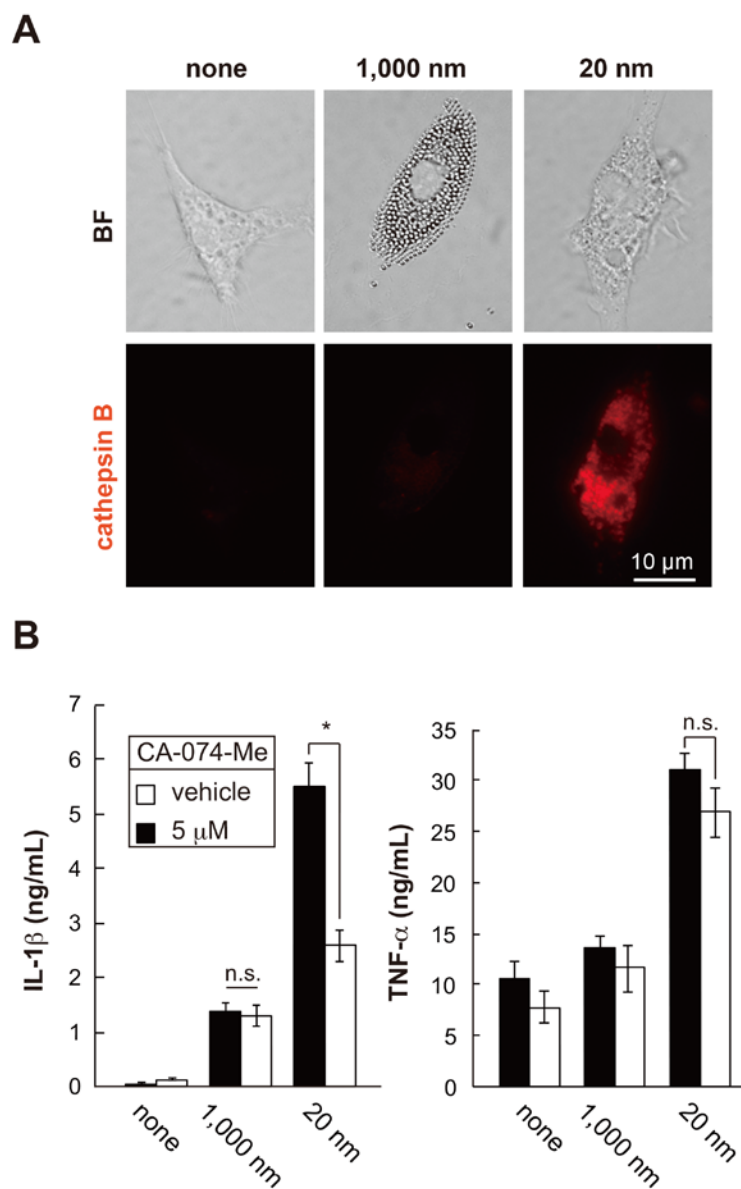
Production of TNF- $\alpha$  and MCP-1 was analyzed by a cytometric bead array as described in Figure 2b. Bar graphs show the mean (SD) of triplicate cultures.



**Supplementary Fig. 3. Interleukin-1 $\beta$  production by bone marrow-derived macrophages in response to amyloid  $\beta$  preparations and lipopolysaccharide.**

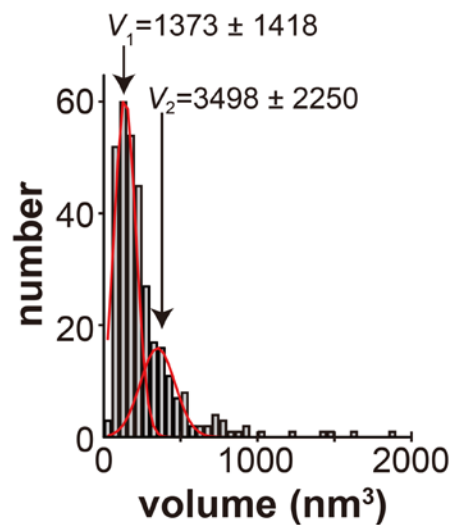
Bone marrow-derived macrophages were stimulated with an amyloid  $\beta$  oligomer or

fibril preparation in the presence of lipopolysaccharide. After 24 h, interleukin-1 $\beta$  (IL-1 $\beta$ ) production was analyzed by ELISA. The bar graph shows the mean (SD) of triplicate cultures.



**Supplementary Fig. 4. Cathepsin B-dependent interleukin-1 $\beta$  production by microglia in response to 20 or 1,000 nm latex beads.**

(A) Microglia on coverslips were cultured with 20 or 1,000 nm latex beads in the presence of lipopolysaccharide (LPS) for 24 h and then incubated with a fluorescent cathepsin B substrate for the last 20 min of culture. (B) After treatment with the cathepsin B inhibitor CA-074-Me for 1 h, microglia were stimulated with 20 or 1,000 nm latex beads in the presence of LPS for 9 h in a stirred culture. Production of IL-1 $\beta$  and TNF- $\alpha$  was analyzed by ELISA and cytometric bead array, respectively. The bar graphs show the mean (SD) of triplicate cultures. BF, bright field; n.s., non-sense; \*  $p < 0.01$  ( $t$ -test).



**Supplementary Fig. 5. Volume distribution of cross-linked oligomers in AFM analyses**

Volume distribution of cross-linked A $\beta$  oligomers from Figure 4 that were larger than 428 nm<sup>3</sup> (~225 kDa)

## References

- [1] T. Adachi, K. Takahara, J. Taneo, Y. Uchiyama, K. Inaba, Particle size of latex beads dictates IL-1beta production mechanism, PLoS One 8 (2013) e68499.
- [2] S.W. Schneider, J. Larmer, R.M. Henderson, H. Oberleithner, Molecular weights of individual proteins correlate with molecular volumes measured by atomic force microscopy, Pflugers Arch., EJP 435 (1998) 362-367.